Angular dependence of coercivity in Nd-Fe-B sintered magnets: Proof that coherent rotation is not involved

F. Cebollada,* M. F. Rossignol, and D. Givord
Laboratoire Louis Néel, CNRS 166X, 38042 Grenoble, France

V. Villas-Boas
Instituto de Física, Universidade de Sao Paulo, Caixa Postal 20516, 01498 Sao Paulo, Sao Paulo, Brazil

J. M. González
Instituto de Ciencia de Materiales, Consejo Superior de Investigaciones Científicas, Serrano 144, 28006 Madrid, Spain
(Received 5 June 1995; revised manuscript received 3 August 1995)

An experimental procedure is presented which allows the analysis of the angular dependence of the coercivity of polycrystalline samples $H_c(\theta)$ in terms of the angular dependence of the switching field of the individual grains forming the material, $H_s(\theta')$. The method is based on the measurement of the remanence curves corresponding to three different field configurations (in which the demagnetizing field is directed antiparallel, perpendicular, and almost parallel to the saturating field, respectively). By using this procedure we have studied the angular dependence of the coercivity in sintered oriented magnets based on the $Nd_2Fe_{14}B$ hard phase. According to our results the switching field of the individual crystallites increases monotonically from approximately $0.15H_A$, H_A being the anisotropy field, for those whose easy axis is oriented parallel to the demagnetizing field ($\theta'=0°$), to values close to H_A, for those whose easy axis is perpendicular ($\theta'=90°$), and follows closely a $1/\cos\theta'$ law up to $\theta'=50°$. This shows that the magnetic anisotropy value in the regions where the nucleation takes place during the reversal of magnetization is not far from the bulk value, and also that coherent rotation is not the determinant mechanism among those governing the nucleation process.

I. INTRODUCTION

Coercivity is one of the most important properties of hard magnetic materials form the point of view of their technological utilization[1] and, therefore, the understanding of coercivity mechanisms is a permanent challenge for researchers involved in studying the extrinsic properties of these materials.[2]

For anisotropic, perfectly homogeneous and perfectly oriented polycrystalline magnets based on noninteracting particles, the coercive force H_c should be equal to the anisotropy field H_A. It is well known,[3,4] however, that the coercive force actually measured in permanent magnet materials is typically one order of magnitude lower than the anisotropy field. It is basically accepted that the origin of this discrepancy lies in the distribution of local alterations of the magnetic properties due to a variety of microstructural features giving rise to magnetization reversal though a process which includes a succession of mechanisms, as well as in the role played by interactions, either dipolar and/or exchange, during demagnetization. In the case of R-Fe-B permanent magnet materials (R=Nd or Pr) several such mechanisms which have been proposed can account for the measured order of magnitude of H_c.[4–8] It is, however, not yet well established which one of them is actually responsible for magnetization reversal. As is clear, progress in the understanding of the influence of the microstructural features on the magnetization reversal mechanism of this relevant family of materials is of major interest in order to achieve its optimization.

Experimental analysis combined with analytical or numerical modeling of the possible mechanisms is the way by which this situation can be clarified. In particular, the analysis of the angular dependence of coercivity, $H_c(\theta)$, the angle θ being defined in Fig. 1, appears to be a crucial tool in this context. In the literature, only two mechanisms are generally considered, "nucleation" and "pinning," which are associated with qualitatively different behaviors of $H_c(\theta)$ (Fig. 2). The former, nucleation, is most of the time identified as a uniform coherent rotation mechanism and then gives rise to a $(\cos^{2/3}\theta+\sin^{2/3}\theta)^{3/2}$ behavior for $H_c(\theta)$, according to the Stoner-Wohlfarth model; the latter, pinning, gives rise to the

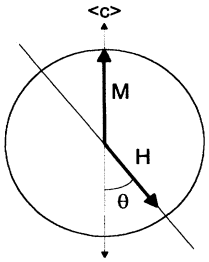

FIG. 1. Conventional geometrical configuration for the study of $H_c(\theta)$ in sintered oriented magnets: The sample is saturated along its easy axis $\langle c\rangle$ and the reversing field **H** is applied at an angle θ with respect to $\langle c\rangle$, and π-θ with respect to **M**. The field for which the maximum of the differential susceptibility in the demagnetization curve appears is taken as $H_c(\theta)$.

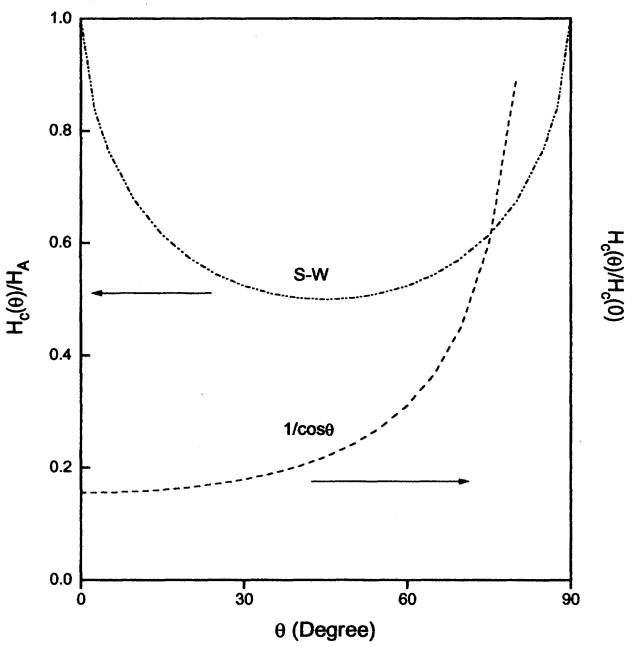

FIG. 2. Angular dependence of the coercivity associated with magnetization reversal through coherent rotation (S-W): The coercive force varies between H_A and $0.5H_A$, presenting a minimum at $\theta=45°$. When coercivity is governed by hindrances to wall expansion or displacement, the coercive force at low θ angles is well below H_A and a $1/\cos\theta$ law is expected.

$1/\cos\theta$ law (sometimes called Kondorski law).[5–11]

To experimentally determine $H_c(\theta)$, a "conventional procedure" consists of saturating the sample along its macroscopic easy axis $\langle c\rangle$ and then measuring the demagnetization curve by applying the field at an angle π-θ from $\langle c\rangle$ (see Fig. 1). H_c is the field value for which the maximum of the susceptibility of the demagnetization curve is observed. However, due to the fact that the intrinsic angular dependence of coercivity in individual grains is smeared out by the angular distribution of crystallite orientations, this conventional procedure provides results whose interpretation is to some extent ambiguous.

This is the case for sintered $Nd_2Fe_{14}B$-based permanent magnets, where $H_c(\theta)$ experimentally obtained generally consists of relatively small and monotonic variations of $H_c(\theta)/H_c(0)$ (see Fig. 3 for example).[10–14] This has been shown[11] to be consistent with a $1/\cos\theta$ dependence of the coercive force in individual crystallites when the angular distribution of crystallite orientations is taken into account. However, in these magnets, free domain wall motion is observed in the thermally demagnetized state, and it is well admitted that this implies that pinning is not involved in the hindrance to magnetization reversal and everyone considers that the coercivity process is nucleation. Considering nucleation, Kronmuller *et al.*[10,12] claim that the observed angular dependence would correspond to Stoner-Wohlfarth behavior which would be strongly altered, either due to the influence of higher-order anisotropy constants and/or to the influence of interactions between grains.

It thus appears that more thorough experimental analysis of the angular dependence of coercivity in permanent magnets is required to clarify the above ambiguity. For this purpose, an approach is presented in this paper which is based upon (i) separating the irreversible from the reversible processes through measurements of remanent magnetization and (ii) selecting the population of grains possibly involved in reversal by means of different geometrical configurations for the saturating and reversing fields. Similar approaches have been proposed in the last years.[15]

The procedure here developed allows the experimental results to be analyzed in terms of the angular dependence of

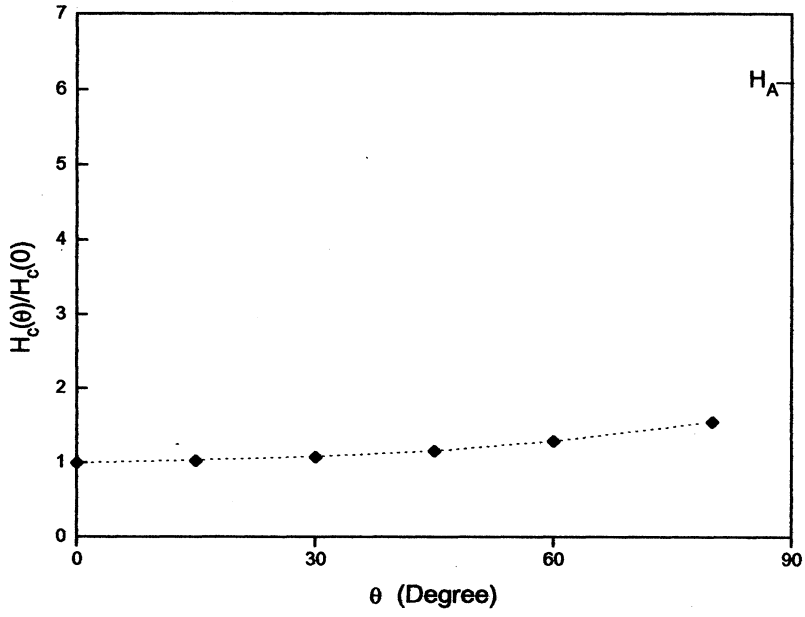

FIG. 3. Angular dependence of the coercivity of the Ugistab magnet measured according to the conventional procedure. Coercivity increases by a factor less than 2 when approaching $\theta=90°$ and is always one order of magnitude lower than the anisotropy field H_A.

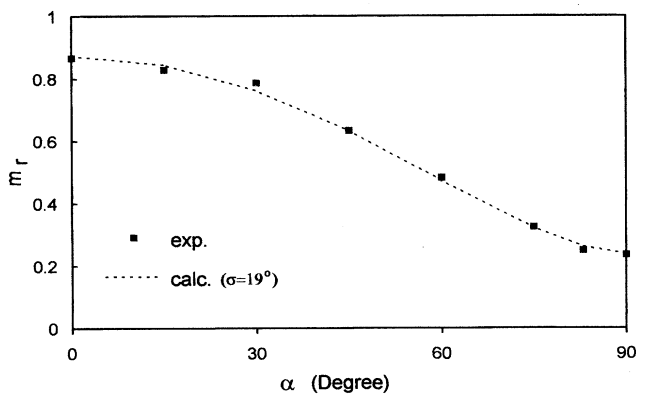

FIG. 4. Reduced remanence measured along a direction at an angle α, with respect to $\langle c \rangle$. Previous saturation of the sample was carried out by applying the field along the direction also given by α. The calculated curve, by using a dispersion given by $\sigma = 19°$, is also shown.

the individual crystallite switching field $H_s(\theta')$. We denote H_s the field at which a given population of grains (situated at the same angle π-θ' from the applied field) reverses its magnetization; as previously, the coercive field H_c concerns all the grains as a whole and is defined by the maximum of the susceptibility in the demagnetization curve.

II. EXPERIMENTAL TECHNIQUES AND SAMPLE CHARACTERIZATION PROCEDURE

Sintered oriented magnets of composition $Nd_{15}Fe_{67.5}B_8Co_5V_4Al_{0.5}$ (Ugistab) were provided by Aimants Ugimag S.A. The samples were cut in the form of disks, 5 mm in diameter and 2 mm thick, by means of spark erosion, with their macroscopic easy axis $\langle c \rangle$ kept in plane. The magnetic measurements were carried out by means of an extraction magnetometer at 175 and 300 K. The magnetic field, also applied parallel to the disk plane, was generated by a superconducting coil up to a maximum of 8 T. The sample holder allowed the sample to be rotated around an axis perpendicular to the disk plane in such way that the angle between the $\langle c \rangle$ axis and the field direction could be adjusted.

A. Characterization of the texture of the samples

In order to determine the sample texture a simple procedure has been developed. The sample is saturated at an angle α from $\langle c \rangle$ by applying an 8-T field along this direction. The field is then removed and the component of the remanent magnetization, $M_r(\alpha)$, along this direction is measured. The plot of the α component of the reduced remanent magnetization, $m_r(\alpha) = M_r(\alpha)/M_s$, as a function of α is shown in Fig. 4.

The analysis of this plot was carried out by considering that, at remanence, the magnetization of each of the crystallites in a sample is directed along its easy axis c. The global remanent magnetization results from the crystallite c-axis

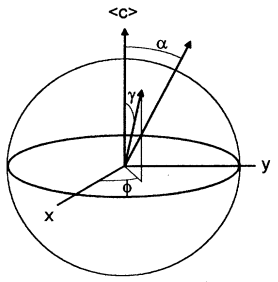

FIG. 5. Scheme of the angle definitions employed for the determination of the texture of the samples.

distribution with respect to $\langle c \rangle$. By assuming that this distribution is given by a Gaussian one of width σ, one can write[11,16]

$$dN(\gamma,\phi) = A \exp[-\gamma^2/2\sigma^2]\sin\gamma \, d\gamma \, d\phi, \tag{1}$$

where $dN(\gamma,\phi)$ represents the percentage of crystallites whose c axes are along the direction given by γ and ϕ (see Fig. 5). The reduced remanent magnetization component was derived in the Appendix and may be written as

$$\begin{aligned} m_r(\alpha) = & \int_{\gamma=0}^{\pi/2}\int_{\phi=0}^{2\pi}[\sin\alpha \sin\gamma \sin\phi + \cos\alpha \cos\gamma]dN(\gamma,\phi) \\ & -2\int_{\gamma_\phi}^{\pi/2}\int_{\phi=-\pi}^{0}[\sin\alpha\sin\gamma\sin\phi \\ & +\cos\alpha \cos\gamma]dN(\gamma,\phi), \end{aligned} \tag{2}$$

with

$$\gamma_\phi = \arctan\left(\frac{-1}{\tan(\alpha)\sin(\phi)}\right). \tag{3}$$

The experimental points can be fitted to expression (2). The obtained value of the fitting parameter is $\sigma = 19°$ (Fig. 4), which agrees with the values measured in similar samples by means of x-ray-diffraction analysis.[16] From this value it can be inferred that almost 100% of the crystallite c axes are oriented within a cone whose half-angle is 60°.

B. Conventional $H_c(\theta)$ measurement

$H_c(\theta)$ was initially measured according to the conventional procedure described above. It increases monotonically with θ (Fig. 3). Due to the fact that the measured magnet is formed of an assembly of crystallites with easy c axes distributed around $\langle c \rangle$, it can be reasonably assumed that the coercive field is minimum for crystallites whose magnetization is precisely antiparallel to H and that it increases as the angle between the crystallite magnetization and H decreases.

III. ANGULAR DEPENDENCE OF THE SWITCHING FIELD: RESULTS AND ANALYSIS

A. Principle

Consider the case of a sample that is in its remanent state after being previously saturated. Assume that a reversed field H_{rev} is applied an angle π-θ with respect to the remanent

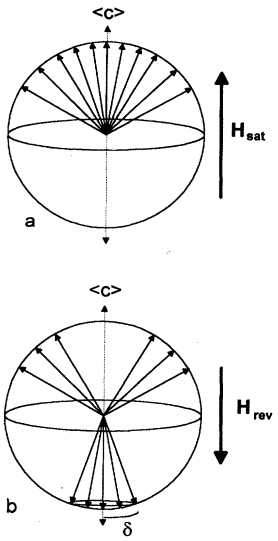

FIG. 6. Configuration A: distribution of the moments at remanence after initial saturation (a) and after application of a reversing field $H_{rev}<H_{sat}$ antiparallel to the remanent magnetization (b).

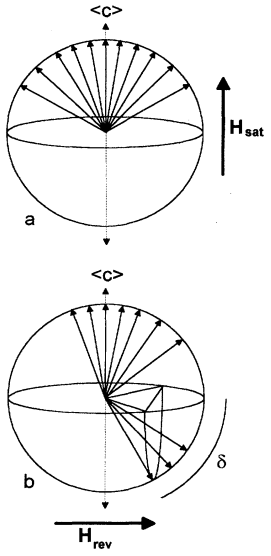

FIG. 7. Configuration B: distribution of the moments at remanence after initial saturation (a) and after application of a field $H_{rev}<H_{sat}$ along the perpendicular to $\langle c\rangle$ (b).

magnetization (see Fig. 1). Two types of processes may take place, either simultaneously or alternatively. First, the moments of some crystallites may reversibly rotate towards the field direction and return to their original orientation after removing the field. Second, the moments of some other crystallites may irreversibly rotate and then adopt an orientation which is antiparallel to the initial one after removing the field. The field H_s required in order to induce such irreversible rotation for a crystallite (the switching field) is strongly dependent on the angle θ' between its c axis and the applied field.

The experimental procedure we have developed to measure $H_s(\theta')$ is based on the assumption that the distribution of the switching fields is essentially determined by the distribution of grain orientations. Since we intend to study the specific population of crystallites whose moments are irreversibly switched upon application of a given H_{rev} field, we must disregard those moments that rotate reversibly, i.e., that return to their initial orientation after taking H_{rev} back to zero. To this end one must separate the reversible from the irreversible changes occurring along the demagnetization curve, which can be achieved by measuring M_r as a function of H_{rev}, i.e., the remanent magnetization after removing H_{rev}.

B. Experimental conditions

Due to the fact that the samples are highly textured, several different configurations of (i) saturating and (ii) reversing fields must be used in order to obtain sufficient information about the angular dependence of the switching field in the whole θ' range, between 0° and 90°. Three of them are particularly useful. They are described in the following.

(i) Configuration A: It consists of saturating the magnetization along the $\langle c\rangle$ direction and then applying the field H_{rev} in the opposite direction (Fig. 6). The main contribution to the irreversible magnetization changes arises from the reversal of grains which are oriented almost antiparallel to the reversing field and only information about the low θ' region of $H_s(\theta')$ is obtained.

(ii) Configuration B: The saturating field is applied along the $\langle c\rangle$ direction and H_{rev} is perpendicular to $\langle c\rangle$ (Fig. 7). The main contribution to the irreversible magnetization comes, in this case, from grains which are oriented at large angles with respect to H_{rev}. This yields information about the large θ' region of $H_s(\theta')$.

(iii) Configuration C: H_{sat} and H_{rev} are separated by a small angle β (7° was used for the measurements) and both are approximately perpendicular to $\langle c\rangle$ (Fig. 8). This third configuration is used in order to study more accurately the region of the $H_s(\theta')$ curve for θ' values close to 90°. Only the moments situated between the planes respectively perpendicular to the saturation and demagnetization directions, i.e., within a dihedral angle of β, contribute to the measured irreversible magnetization.

C. Analysis

(i) When using configuration A, the sample was initially saturated along its macroscopic easy axis $\langle c\rangle$ and, after re-

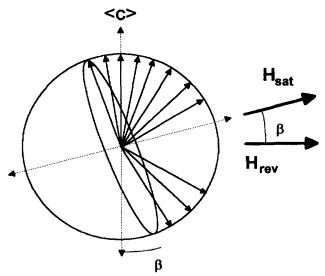

FIG. 8. Configuration C: saturating and reversing fields are almost parallel. Only those moments that, after saturation, were situated between the planes respectively perpendicular to H_{sat} and H_{rev} will contribute to the irreversible magnetization jumps.

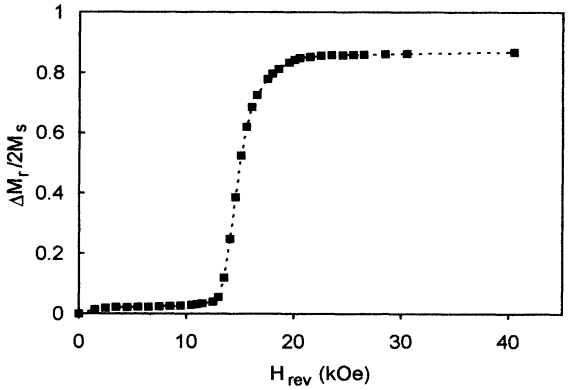

FIG. 9. Configuration A: $\Delta M_r/2M_s$ vs H_{rev} plot corresponding to the measurements carried out at 300 K.

moving the field, the distribution of moments became similar to that shown in Fig. 6(a), exhibiting a certain remanence value M_{rmax}. By successively applying and removing increasing reversed fields H_{rev}, the remanence changes, gradually, from $+M_{rmax}$ to $-M_{rmax}$. The variation of remanence, normalized to $2M_s$ and in absolute value, $\Delta M_r/2M_s$, was measured as a function of H_{rev}, the result shown in Fig. 9 corresponding to 300 K. No increase is observed for fields less than 1.3 T approximately. This field marks the first reversal of some of the moments towards H_{rev}. For fields greater than 2.5 T, the remanent magnetization saturates. This indicates that all the moments of the sample are now reversed.

Considering the fact that $H_s(\theta')$ increases monotonically with θ', it can be assumed that, for a given H_{rev}, all the reversed moments lie within a cone around $\langle c\rangle$ of a given half-angle δ which increases with H_{rev}. The remanent moment configuration, obtained after removing the field, is then similar to that shown in Fig. 6(b) and the value of $\Delta M_r/2M_s$ can be easily calculated by means of the expression

$$\Delta M_r(\delta)/2M_s = \int_{\phi=0}^{\phi=2\pi}\int_{\gamma=0}^{\gamma=\delta} dN(\gamma,\phi)\cos\gamma. \qquad (4)$$

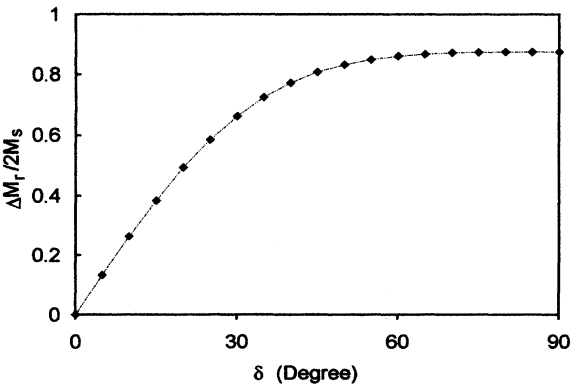

FIG. 10. Calculated values of $\Delta M_r/2M_s$ as a function of δ for $\sigma = 19°$.

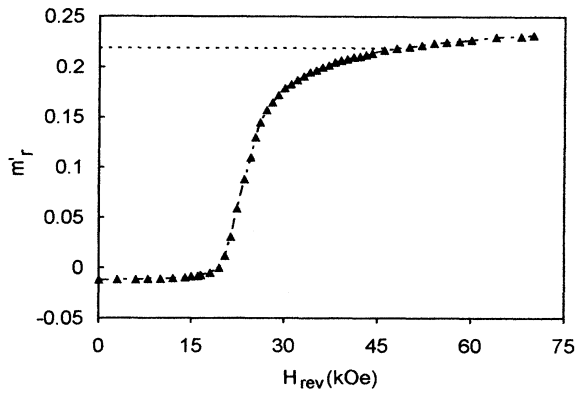

FIG. 11. Reduced remanence M_r/M_s as a function of H_{rev} for the measurements carried out at 300 K according to configuration B. When configuration C was employed no increase in the remanence was observed (horizontal dotted line) until fields close to 47 kOe were reached; for higher fields, the remanence increased according to the curve measured by means of configuration B.

The calculated $\Delta M_r(\delta)/2M_s$ curve for a dispersion $\sigma = 19°$ is shown in Fig. 10. It reaches saturation at approximately $\delta = 60°$, as expected.

From a comparison between the experimental $\Delta M_r(H_{rev})/2M_s$ and calculated $\Delta M_r(\delta)/2M_s$ curves (Fig. 9 and Fig. 10, respectively) it is possible to deduce the field required to reverse those crystallites whose axes are oriented at an angle θ' from $\langle c\rangle$. As an example, when the moments of all the crystallites whose c axes are contained within a cone of half-angle $\delta = 26°$ have been reversed, the calculated value of $\Delta M_r/2M_s$ is 0.6. Such a value is reached for a field of 1.55 T, and thus the value of H_s for $\theta' = 26°$ is obtained.

Since there are almost no crystallites whose c axes are separated by more than 60° from $\langle c\rangle$, only the $\theta' < 60°$ portion of the $H_s(\theta')$ curve can be determined with sufficient accuracy using configuration A. For the $\theta' > 60°$ portion of the curve, configurations B and C must therefore be used.

(ii) In the case of configuration B (Fig. 7), upon saturating the sample along the $\langle c\rangle$ direction and removing the field, the configuration of the moments is similar to that shown in Fig. 7(a), which yields a remanent magnetization, measured along the H_{rev} direction, equal to zero. The remanence was measured after successively applying and then removing increasing H_{rev} fields. In this case, only the moments in the left hemisphere may irreversibly jump to the right, towards the field direction, increasing the remanence (always measured along the H_{rev} direction). As shown in Fig. 11, the reduced remanent magnetization m_r' suddenly increases from a value near zero to a certain value m_r' at a field close to 2 T. Fields over 7.5 T are required to reach complete saturation of m_r'. Such field value is very close to H_A (8.5 T).

For this configuration, again assuming that $H_s(\theta')$ is a monotonous function, the reduced remanent magnetization along H_{rev} is given by

$$m_r'(\delta) = \int_{\phi=0}^{\Phi=\pi}\int_{\gamma=\gamma_\phi}^{\gamma=\pi/2} 2\,\sin\gamma\,\sin\phi\; dN(\gamma,\phi), \qquad (5)$$

with

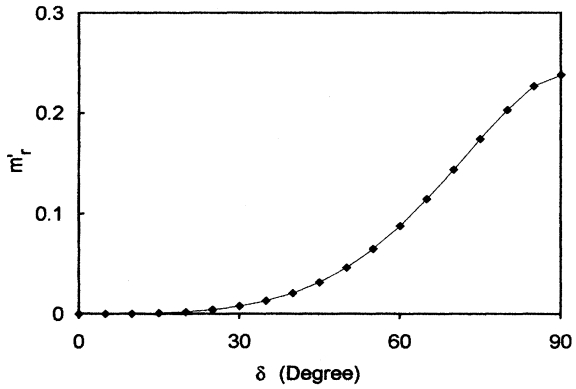

FIG. 12. Calculated values of $m_r'(\delta)$ for $\sigma=19°$.

$$\gamma_\phi = \arcsin[-\sin\delta/\sin\phi]. \quad (6)$$

The calculated $m_r'(\delta)$ values are plotted in Fig. 12 (for $\sigma=19°$, as above). No increase is observed until values of $\delta=30°$ are reached. This again is in agreement with the fact that most of the c axes of the individual crystallites are confined inside a cone, where the axis is $\langle c\rangle$ and the half-angle of the order of 60°.

According to the calculation, $m_r'=0.2$ corresponds to all the crystallites within a cone of $\delta=79°$ having reversed magnetization. The experimental curve indicates that $H_{\rm rev}=3.6$ T is required for this to be fulfilled. Configuration B enables only the $\theta>50°$ portion of $H_s(\theta')$ to be studied.

(iii) For the case of configuration C, the magnetic moments close to $\theta'=90°$ can be studied with more accuracy than before. Irreversible effects are only observed for $H_{\rm rev}$ greater than 4.7 T. This confirms that fields approaching the anisotropy field are needed to reverse these moments.

(iv) Synthesis: Figure 13 presents the $H_s(\theta')$ curves obtained, at 175 and 300 K, by assembling all the data from the measurements carried out in the different configurations A, B, and C. The curve corresponding to 300 K shows a continuous increase from 1.3 T, for $\theta'=0$, up to values close to

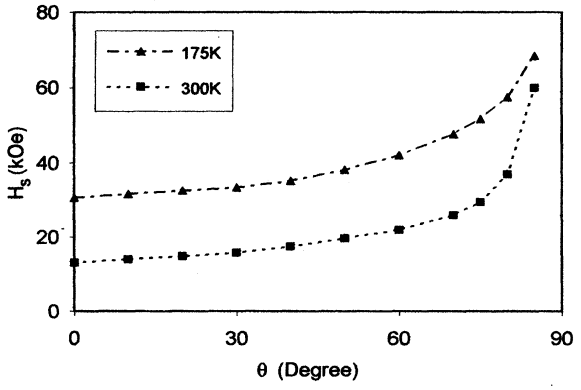

FIG. 13. Angular dependence of the switching field of the individual crystallites, $H_s(\theta')$, corresponding to measurements at 300 and 175 K.

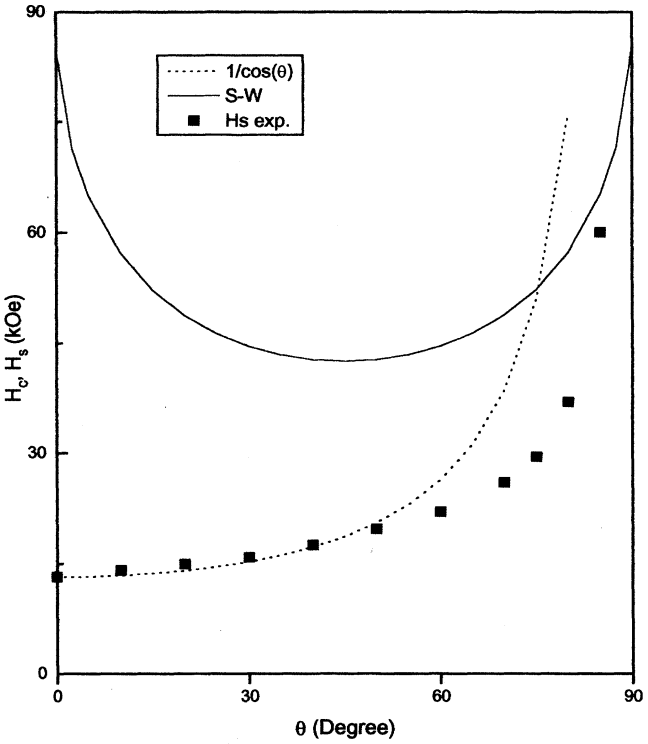

FIG. 14. Comparison of the $H_s(\theta')$ curve, experimentally obtained at 300 K, with the $1/\cos\theta$ law and with the behavior associated with coherent rotations (S-W). As observed, the switching field of the individual crystallites exhibits a $1/\cos\theta$ behavior up to almost $\theta=50°$.

the anisotropy field when approaching $\theta'=90°$. The normalized coercive field $H_s(\theta')/H_s(0)$ then reaches values as high as 6. Measurements at 175 K showed a similar behavior. The coercive field at this temperature is 2.5 larger than at 300 K and the available field was not sufficiently high (8 T maximum) to study the full $H_s(\theta')$ curve.

IV. DISCUSSION OF RESULTS AND CONCLUDING REMARKS

The contribution of the individual crystallites to the irreversible susceptibility has been determined by making the following assumptions: (i) The coercive field distribution is uniquely determined by the distribution of grain orientations, and (ii) the monotonic increase in $H_c(\theta)$ implies that the $H_s(\theta')$ curve is increasing monotonically with θ'.

Our analysis shows that the individual crystallites switching field, H_s, increases monotonically from approximately $0.15H_A$ to values close to H_A and follows closely a $1/\cos\theta'$ law up to θ' values around 50° (Fig. 14). This indicates that for such moments, the torque due to the applied field is not sufficient to induce a significant moment rotation. For $\theta'>50°$, the applied field required for moment reversal approaches the anisotropy field: The torque is now sufficient to induce a rotation and the system tends to coherent rotation.

If we take into account that nucleation mechanisms usually considered in Nd-Fe-B magnets associate the reduction

of the coercive force to the presence, in real materials, of regions where the anisotropy and/or exchange constants differ significantly from the values corresponding to the hard phase, the field required to achieve the local reversal of magnetization at these regions is lower than that needed where the properties of the hard phase are preserved. Due to this local magnetic softness, a certain rotation of the moments must occur prior to magnetization reversal, which allows one to consider that coherent rotation (as described by the Stoner-Wohlfarth model) is involved in magnetization reversal.[4,6] Then, $H_c(\theta)$ curves qualitatively similar to that shown in Fig. 2 are expected.

According to the results, the $H_s(\theta')$ curves of sintered Nd-Fe-B magnets exhibit a behavior qualitatively different from that expected when coherent rotation is involved (Fig. 14). These results confirm the interpretation of the angular dependence of coercivity in these magnets which has already been proposed. This throws light on the understanding of coercivity in these systems. In particular, it is now clear (i) that coherent rotation (as described by the Stoner-Wohlfarth model) is not the determinant mechanism among those brought into play in the nucleation process and (ii) that the anisotropy value governing the magnetization reversal is close to the bulk value.

A large variation in the $H_s(\theta')/H_s(0)$ ratio was observed, from 1.0 to almost 6.5, as compared with smaller values measured by means of the conventional procedure (see Fig. 3), which is described in the Introduction section and in Fig. 1. A simple argument may explain why the latter yields very small values for $H_c(\theta)/H_c(0)$. When a sample is saturated along its $\langle c \rangle$ axis and a perpendicular demagnetizing field is applied, $H_c(90°)$ is taken as the field for which the maximum of the irreversible susceptibility occurs. However, the component along the field direction of those moments that are oriented at angles much lower than 90° with respect to the applied field is much larger than that due to the moments oriented at almost 90° (that is, almost parallel to the $\langle c \rangle$ axis). The contribution to the irreversible susceptibility due to the moments oriented at angles much lower than 90° may easily overcome that due to those oriented at almost 90°. In this way the measured value of $H_c(90°)$ is much lower than the corresponding to an individual crystallite oriented at 90° with respect to the applied field.

Regarding exchange interactions between neighboring grains (usually considered as the origin of enhanced remanence in nanostructured melt spun Nd-Fe-B materials[17,18]), we may expect that the remanence in our samples is essentially determined by the orientation of the easy axes of each crystallite since the exchange length in these materials is of a few nanometers, that is, about three orders of magnitude lower than their grain size (of the order of 10 μm).[18] Nevertheless, these interactions may alter the fields required for magnetization reversal,[7] although the monotonous increase of $H_c(\theta)$ when measured by means of the conventional procedure makes our basic assumptions feasible.

Finally, it is important to note that the assumption in our analysis [i.e., $H_s(\theta')$ increases monotonically with θ'] is not applicable to all magnets. In the case of magnets with nonmonotonic conventional $H_c(\theta)$ curve, the determination of the remanent magnetization with respect to the only H_{rev} field is not sufficient and more complex measurement methods are to be used. This is, for example, the case of single-domain ferrite magnets or $Pr_2Fe_{14}B$-based magnets measured at low temperatures,[15,19] for which the conventional $H_c(\theta)$ curve is not monotonic but presents a minimum near $\theta=45°$, which appears to be noncompatible with the assumption of progressive reversal of the moments from 180°. We are currently developing a suitable experimental method to treat this particular case.

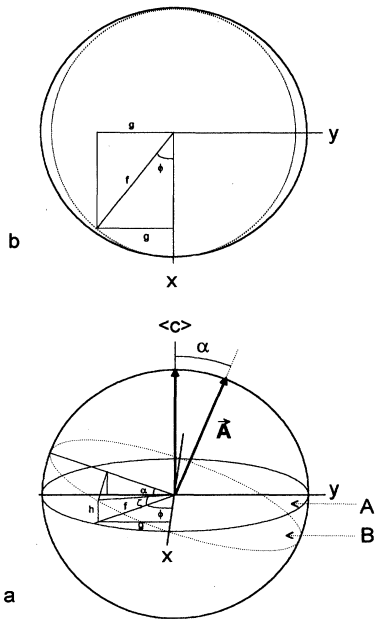

FIG. 15. Scheme of the angle definitions employed for deriving Eq. (2) in the Appendix (a) and projection of the figure on the xy plane (b).

ACKNOWLEDGMENTS

This work was partly supported by the Commission of the European Communities within the Concerted European Action on Magnets and by the Comunidad Autónoma de Madrid.

APPENDIX

Considering a sample whose macroscopic easy axis $\langle c \rangle$ points in the z direction, the reference frame being that shown in Fig. 5, the orientation of the particular c axis of any crystallite can be expressed by means of the unit vector

$$\mathbf{U}_c=(\sin\gamma\cos\phi,\sin\gamma\sin\phi,\cos\gamma), \tag{A1}$$

while the α direction is given by a vector

$$\mathbf{A}=(0,\sin\alpha,\cos\alpha). \tag{A2}$$

The component along the α direction of the remanent moment of a crystallite can be obtained through the projection of $\mathbf{U}_c$ over $\mathbf{A}$, given by the product

$$\mathbf{U}_c\mathbf{A}=\sin\alpha\sin\gamma\sin\phi+\cos\alpha\cos\gamma. \tag{A3}$$

When a saturating field is applied along the positive $\langle c \rangle$ axis and then removed, the remanent magnetic moments of all crystallites will be contained in the upper hemisphere defined by plane A in Fig. 15(a), each one pointing along its particular c axis. To calculate the remanent magnetization measured along the α direction, $m_r^*(\alpha)$, we should consider the components of all moments

$$m_r^*(\alpha)=\int_{\gamma=0}^{\pi/2}\int_{\phi=0}^{2\pi}[\sin\alpha\,\sin\gamma\,\sin\phi + \cos\alpha\,\cos\gamma]dN(\gamma,\phi), \tag{A4}$$

where $dN(\gamma,\phi)$ represents the percentage of crystallites whose c axes are along the direction given by γ and ϕ.

However, if a saturating field is applied along the direction given by **A** and then removed, all remanent moments will point in the upper hemisphere defined by plane B (perpendicular to vector **A**), each one along its particular c axis. This means that the moments initially placed in the left region defined by planes A and B, i.e., within a dihedral angle of α, will be shifted to the (symmetric) right region. We have to consider that the reduced remanence now measured, $m_r(\alpha)$, is

$$m_r(\alpha)=m_r^*(\alpha)-2\Delta, \tag{A5}$$

where 2Δ is the remanence change due to the contribution of the moments initially contained inside the left region. In order to calculate this contribution, we must know the integration limits corresponding to this region, for which the aid of the angle definitions of Fig. 15 is required. To cover it, the angle ϕ must go from $-\pi$ to 0 and γ will vary from $(\pi/2)-\zeta$ to $\pi/2$, the angle ζ being dependent on ϕ. In particular, when $\phi=-\pi/2$, ζ is equal to α, while for $\phi=0$ and $\phi=-\pi$, ζ is equal to $\pi/2$. The relation linking ζ and ϕ can be obtained by considering (see Fig. 15) that

$$\tan(\zeta)=h/f, \tag{A6}$$

$$\tan(\alpha)=h/g, \tag{A7}$$

$$\sin(\phi)=-g/f\ ; \tag{A8}$$

then

$$\tan(\zeta)=-\tan(\alpha)\sin(\phi) \tag{A9}$$

and

$$\zeta=\arctan[-\tan(\alpha)\sin(\phi)]. \tag{A10}$$

Thus the integration limits for γ must go from γ_ϕ to $\pi/2$, with

$$\gamma_\phi=(\pi/2)-\zeta=\arctan\left(\frac{-1}{\tan(\alpha)\sin(\phi)}\right). \tag{A11}$$

Then Eq. (A5) can be written as

$$m_r(\alpha)=\int_{\gamma=0}^{\pi/2}\int_{\phi=0}^{2\pi}[\sin\alpha\,\sin\gamma\,\sin\phi+\cos\alpha\,\cos\gamma]dN(\gamma,\phi) -2\int_{\gamma_\phi}^{\pi/2}\int_{\phi=-\pi}^{0}[\sin\alpha\,\sin\gamma\,\sin\phi + \cos\alpha\,\cos\gamma]dN(\gamma,\phi), \tag{A12}$$

which corresponds to the reduced remanent magnetization component along the direction given by **A**, that is, to Eq. (2).

*Permanent address: Instituto de Ciencia de Materiales, CSIC, Serrano 144, 28006 Madrid, Spain.

[1] H. Kronmüller, Phys. Status Solidi B **144**, 385 (1987).
[2] D. Givord, M. F. Rossignol, and D. W. Taylor, J. Phys. (Paris) Colloq. **2**, C3-95 (1992).
[3] M. Sagawa, S. Fujimura, N. Tagawa, and Y. Matsuura, J. Appl. Phys. **55**, 2083 (1984).
[4] H. Kronmüller in *Science and Technology of Nanostructured Magnetic Materials*, edited by G. C. Hadjipanajis and G. A. Prinz (Plenum, New York, 1991), p. 657.
[5] D. Givord, Q. Lu, and M. F. Rossignol, in *Science and Technology of Nanostructured Magnetic Materials,* edited by G. C. Hadjipanajis and G. A. Prinz (Plenum, New York, 1991), p. 635.
[6] H. Kronmüller, in *Supermagnets, Hard Magnetic Materials,* edited by G. J. Long and F. Grandjean (Kluwer Academic, Dordrecht, 1991), p. 461.
[7] J. M. González and F. Cebollada, Jpn. J. Appl. Phys. **33**, 4606 (1994).
[8] R. W. McCallum, A. M. Kadin, G. B. Clemente, and J. E. Keem, J. Appl. Phys. **61** (8), 3577 (1987).
[9] E. C. Stoner and E. P. Wohlfarth, Philos. Trans. R. Soc. London **240**, 599 (1948).
[10] H. Kronmüller, K.-D. Durst, and G. Martinek, J. Magn. Magn. Mater. **69**, 149 (1987).
[11] D. Givord, P. Tenaud, and T. Viadieu, J. Magn. Magn. Mater. **72**, 247 (1988).
[12] H. Kronmüller, K.-D. Durst, and M. Sagawa, J. Magn. Magn. Mater. **74**, 291 (1988).
[13] S. Hirosawa, K. Tokuhara, Y. Matsuura, H. Yamamoto, S. Fujimura, and M. Sagawa, J. Magn. Magn. Mater. **61**, 363 (1986).
[14] F. E. Pinkerton, J. Magn. Magn. Mater. **54-57**, 579 (1986).
[15] S. Wirth and W. Christoph, J. Appl. Phys. **72**, 5358 (1992).
[16] D. Givord, A. Liénard, R. Perrier de la Bâthie, P. Tenaud, and T. Viadieu, J. Phys. (Paris) Colloq. **46**, C6-313 (1985).
[17] G. B. Clemente, J. E. Keem, and J. P. Bradley, J. Appl. Phys. **64**, 5299 (1988).
[18] J. M. D. Coey, J. Magn. Magn. Mater. **140-144**, 1041 (1995).
[19] G. Martinek, H. Kronmüller, and S. Hirosawa, J. Magn. Magn. Mater. **89**, 369 (1990).